Synthesis and optimization of a PEM fuel cell system via reactor-separation network (RSN)

S.K. Kamarudin [a,*], W.R.W. Daud [a], A. Md. Som [b], M.S. Takriff [a], A.W. Mohammad [a]

[a] *Department of Chemical and Process Engineering, Universiti Kebangsaan Malaysia, 43600 UKM Bangi, Selangor, Malaysia*
[b] *Faculty of Chemical Engineering, Universiti Teknologi MARA, 40450 Shah Alam, Selangor, Malaysia*

Abstract

The main objective of this study is to develop the synthesis and optimization of reactor-separation network (RSN) models that can be simultaneously solved within Non-Linear Programming (NLP) for a PEM fuel cell system. The objective function for optimization was defined to minimize the overall cost and CO production. Five alternatives were synthesized to determine the best flow chart for the system based on cost and the output concentration of carbon monoxide. A Polymer Electrolyte Membrane Fuel Cell (PEMFC) system was taken as the case study. The results indicated that the optimum specific cost of a PEMFC stack was found to be in the region of US$ 500–700 kW^{-1}, while the specific manufacturing cost and the specific investment cost were calculated at the range of US$ 1000–1500 and 2500–3000 kW^{-1}, respectively. Furthermore, the infrastructure investment cost was determined to be in the range of US$ 10–30 billion with the specific cost for one unit in the range of US$ 2000–4000 kW^{-1}. The results obtained are comparable with other studies.
© 2005 Elsevier B.V. All rights reserved.

Keywords: Process synthesis; Process optimization; PEMFC; Reactor-separation network (RSN); NLP

1. Introduction

Very few publications exit on the optimization of reactor-separation networks (RSN) although in most chemical processes, reactors are sequenced by separation systems. Most of the research work on optimization only concentrates on the heat management [1–10] and reaction system but the interaction between the structure, design and operation of both reaction and separation units are not fully exploited particularly for a fuel cell system. The limitation of this approach is due to the complexity of the formulation involved in doing so, but these parameters are very important in process system engineering in order to ensure the purity of the final product and to reduce the overall cost as well as waste generation.

2. Problem statement

The problems to be addressed in this paper can be stated as Table 1.

The main objective of this study is to introduce synthesis of the superstructure-based approach to the synthesis of a RSN network For PEM fuel cell system as follows:

- To develop reactors with a continuous reaction and separation system, which are based on Linear Programming (LP) and Non-Linear Programming (NLP) synthesis procedures.
- To develop a simplified and user friendly, yet a general superstructure of RSN networks in matrix form and solved using MATHLAB, and the overall process synthesis/optimization is carried out at different level of superstructure details and model aggregation.

3. Methodology

The optimization problem is considerably more difficult if the variables included take into consideration the integer and binary (0–1) values. These problems are referred to as Mixed Integer Non-linear Programming (MINLP) problems and usually become the hardest part to be solved unless a special structure can be exploited. However, in practice, most design problems are not solved using superstructures and mixed-integer

* Corresponding author. Tel.: +60 3 89216422; fax: +60 3 89216148.
E-mail address: ctie@vlsi.eng.ukm.my (S.K. Kamarudin).

Nomenclature

A	cell active area
A	linear inequality constraints
A_{eq}	linear equality constraints
A_0	pre-exponential factor
A_M	area of membrane
A_A	area of adsorber
A_F	active area of fuel cell
ATR, R1	auto-thermal reformer
c/c_F	degree of purification
c_{eq}	non-linear equality constraints
C	non-linear inequality constraints
C_A	methanol cost
C_B	water supply cost
C_C	oxygen supply cost
C_{R-1}	cost for Reactor 1
C_{R-2}	cost for Reactor 2
C_{R-3}	cost for Reactor 3
C_{R-4}	cost for Reactor 4
C_{S-1}	cost for unit separation 1
C_{S-2}	cost for unit separation 2
$C_M, C_S, C_{O_2}, C_{CO}$	molar concentration for methanol, steam, O_2, CO
$C_{Utilities}$	cost for utilities
CT	total investment cost
D	diameter
E_a	activation energy
F	Faraday constant (96,487 C)
$f(x)$	objective function
F_{MO}	feed concentration of methanol
f_p	cost factor for pressure
f_m	cost factor for material
FC, R5	fuel cell stack
$g(x)$	equality constraints
$h(x)$	inequality constraints
[**H**]	Hessian matrix
i	current
i_0	current density
I_{Cost}	cost index
J	activity of inequality constraints
$k_1, k_2, k_M, k_S, k_{O_2}, k_H, k_{CO}$	reaction constant reaction 1, 2, methanol, steam, oxygen, hydrogen, carbon monoxide
L	length
Lb, X^{low}	lower bound limit
m	number of equations
M_0, M_S	ratio of methanol to hydrogen and steam
MR, R4	membrane reactor
n	number of variables
$n_{fuel\ cell}$	fuel cell efficiency
P	pressure
P_M	partial pressure for methanol
P_{H_2}	partial pressure for hydrogen
POX	partial oxidation
PROX, R3	preferential oxidation
PSA, S2	pressure swing adsorber
Q_1, Q_2, Q_3	heat balance for reactors 1–3
$r_1, r_2, r_M, r_S, r_{O_2}, r_H, r_{CO}$	rate of reaction for reaction 1, 2, methanol, steam, oxygen, hydrogen, carbon monoxide
S_{H_2}	hydrogen selectivity
S	search direction
S_1, S_2, S_3, S_4	selectivity for reactors 1–4
SR	steam reforming
T_0	initial temperature
T_1, T_2, T_3	temperature
TCM, S1	tubular ceramic membrane
Up, X^{up}	upper bound limit
V_{cell}	voltage of single cell (V)
$V, V_1, V_2, V_3, V_{ATR}, V_{WGS}, V_{PROX}$	volume of reactor
w	width
WGS, R2	water gas shift reactor
$x_{F,i}$	mole fraction of component i in feed stream
$x_1, x_2, \ldots, x_n$	design parameters
X_A	conversion of component A

Greek letters

a	step calculation
α^*	ideal separation factor
ε_W	volume expansion factor
η	pore diameter
λ	the conversion of H_2 to H_2O in PROX
θ	degree of separation
ρ	density

optimization algorithms only [11]. In addition, the mixed integer formulation of the optimization problem, in principle, permits the optimizer to select simultaneously the best flow sheet and optimize it with respect to its continuous variables [12,13]. Due to that, in this study the initial stage generations of the RSN

Table 1
Problem statements

Given	Find
Rate of chemical reaction in the reactors	The reactor network (i.e. size of reactors, feeding, conversion of reactants, etc.)
Feed flow rates and composition of feed streams	The separation network strategy (e.g. the size of the membrane and adsorber, and the sequence)
Degree of separation for separators, i.e. membrane and adsorber	The interconnection between the two networks
Physical and chemical properties of components	Selecting the best alternative by synthesizing the RSN based on minimum cost and product purity
A performance criterion (e.g. total cost, yield, selectivity of desired product)	
Mass balance of the system	
Energy balance of the system	

networks are simplified to the Non-Linear Programming (NLP) procedures.

Although the NLP approach is computationally more extensive, it has been proven to be a more robust and reliable method [14–16]. The NLP problems in the study were solved using optimization tools in MATHLAB. MATHLAB is a standard tool introduced for technical computing and was originally developed as a matrix laboratory. The major element of MATHLAB is a matrix. Mathematical manipulations of matrices are very conveniently implemented and easy to-use as an interactive environment. To these matrix manipulations, MATHLAB has added a variety of numerical method functions, symbolic computations and visualization tools [30,31].

SQP has emerged as a very popular and powerful method for solving NLP problems in process optimization [12,15,17]. Fig. 1 summarizes the flow chart for the development of an NLP algorithm for SQP. [**H**] or Hessian matrix is referred to as $\Delta^2 f(X_i)$ and S is referred to as search direction.

Optimization techniques are used to find a set of design parameters, i.e. $x = \{x_1, x_2, \ldots, x_n\}$, that can, in some ways, be defined as optimal. The development of algorithms for synthesis and optimization of the RSN in this study were based on the modified finite difference derivatives in sparse matrix. These algorithms can be used to solve function with multiple variables

with constraints as follows:

$$\text{Minimize } f(x) \tag{1}$$

s.t.

$$c(x) = 0 \tag{2}$$

$$c_{\text{eq}}(x) = 0 \tag{3}$$

$$Ax \le b \tag{4}$$

$$A_{\text{eq}}x \le b_{\text{eq}} \tag{5}$$

$$lb \le x < ub \tag{6}$$

with x, b, b_{eq}, lb and ub are vector in the form of sparse matrix, A and A_{eq} are the sparse matrix returns the values for linear constraints, $c(x)$ and $c_{\text{eq}}(x)$ are the function for non-linear constraints translates the vector and the $f(x)$ is the function that translates in scalar. $f(x)$, $c(x)$ and $c_{\text{eq}}(x)$ are non-linear function.

4. System description

Fig. 2 shows the schematic diagram of a PEMFC system. The main electric power generator in the system is the fuel cell stack (that contains the anode, cathode, PEM and cooling plates) as shown in the diagram. Fuel gas containing H_2 is fed to the anode side and oxygen (or air) is fed to the cathode side of the stack. The spent fuel gas and the gas leaving the fuel cell stack are referred to as the anode exhaust and cathode exhaust, respectively. For convenience in describing the fuel cell system configuration as shown in Fig. 2, the following paragraph and Table 2 shall explain the layout of the system in terms of the flows of oxygen (or air), fuel, processed water, exhaust gases and stack coolant.

Beginning at the right-bottom, ambient air is compressed to 3 atm and passes through an oxygen concentrator to separate the O_2 from N_2. This stream will split into two main streams. The smaller oxygen (or air) flow is preheated and fed to an ATR reactor. On the other hand, the larger oxygen (or air), which flows to the HUM 1, is humidified and cooled by injecting liquid water prior to being supplied to the cathode inlet of the fuel cell stack. The fuel flow circuits begin at the fuel tank (methanol). From the tank, it is pumped to the fuel vaporizer where it is heated and vaporized by the hot stream exhaust gas. It is then fed to the ATR where it reacts with the preheated air and superheated steam to yield the raw reformate. The hot reformate is used to superheat the ATR steam feed. It is then mixed with additional water and fed to a WGS reactor. The fuel gas leaving this reactor will pass through the water adsorber unit. The purpose of this unit is to remove the excess water in the stream before entering the membrane units. The flow that leaves the membrane unit is then cooled by lowering the temperature of the inlet oxygen (or air) and subsequently vaporized the feed methanol to the ATR before entering the adsorber. Finally, the purified hydrogen fuel flow will be humidified to 100% by a HUM 2 and will enter the anode side of the stack.

The exhaust gas circuit is best traced from the upper left corner in Fig. 2. The fuel cell cathode exhaust is cooled to recover
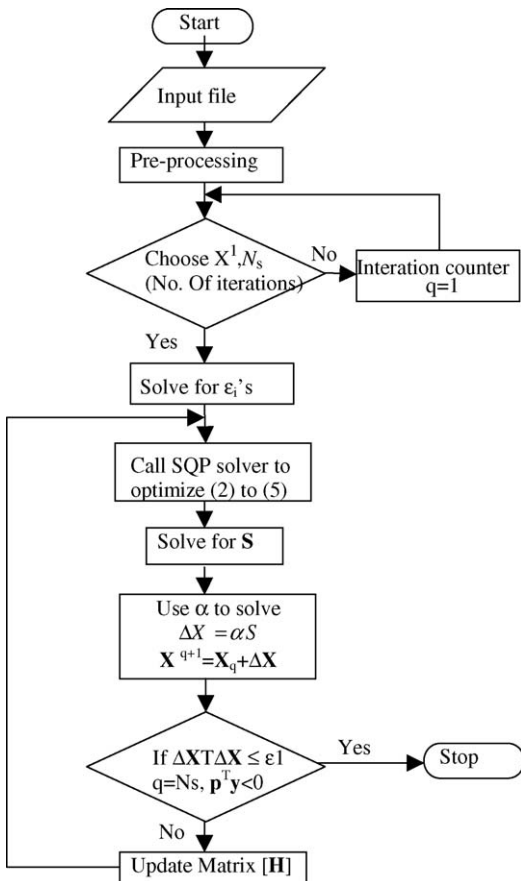

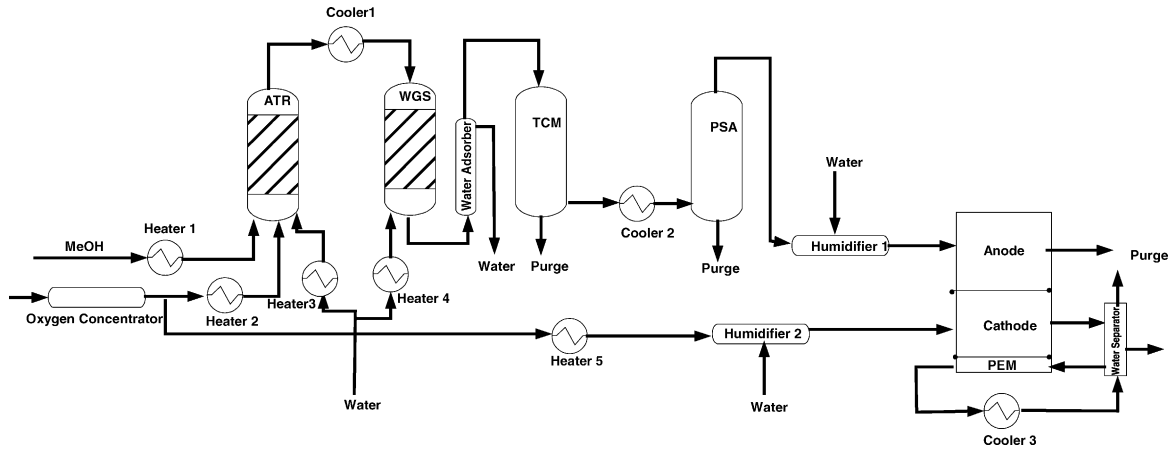Fig. 1. Flowchart of NLP Algorithm for SQP.

Fig. 2. The proposed schematic diagram of PEMFC system in this study.

Table 2
System layout and alternatives

Items	Description	Reaction
Auto-thermal reformer (ATR)	Producing H_2 from methanol (A) and steam (B) with co-feeding with oxygen (C)	Endothermic steam reforming: $CH_3OH + H_2O \rightarrow CO_2 + 3H_2$ exothermic partial oxidation, $CH_3OH + 0.5O_2 \rightarrow CO_2 + 2H_2 + (CO)$
Water gas shift reactor (WGS)	Secondary hydrogen producer and primary CO clean-up system	$CO + H_2O \Leftrightarrow CO_2 + H_2$
Preferential oxidation (PROX)	Alternative to WGS in removing CO	$CO + O_2 \rightarrow CO_2$
Tubular ceramic membrane (TCM) and pressure swing adsorber (PSA)	Operated in parallel to yield the product purity as 99.9% hydrogen and CO less than 20 ppm	
Fuel cell stack (FC)	Consists of three major components; anode, cathode and platinum-catalyzed	Anode: $2H_2 \rightarrow 4e^- + 4H^+$; cathode: $4e^- + 4H^+ + O_2 \rightarrow 2H_2O$
Membrane reactor (MR)	Combines ATR, WGS and TCM	Overall: $2H_2 + O_2 \rightarrow 2H_2O$

water and purged to the air. The last subsystem is the stack coolant circuit that is used to remove the waste heat from the fuel stack. Coolant from the tank is pumped to the cooling plates in the fuel cell stack. The heated coolant then flows to the main radiator and then back to the coolant tank.

5. Model development of RSN network

Fig. 3 shows the alternative configurations of the process units in the system in block diagram superstructure while Fig. 4 shows the superstructure embedded with the five alternatives.
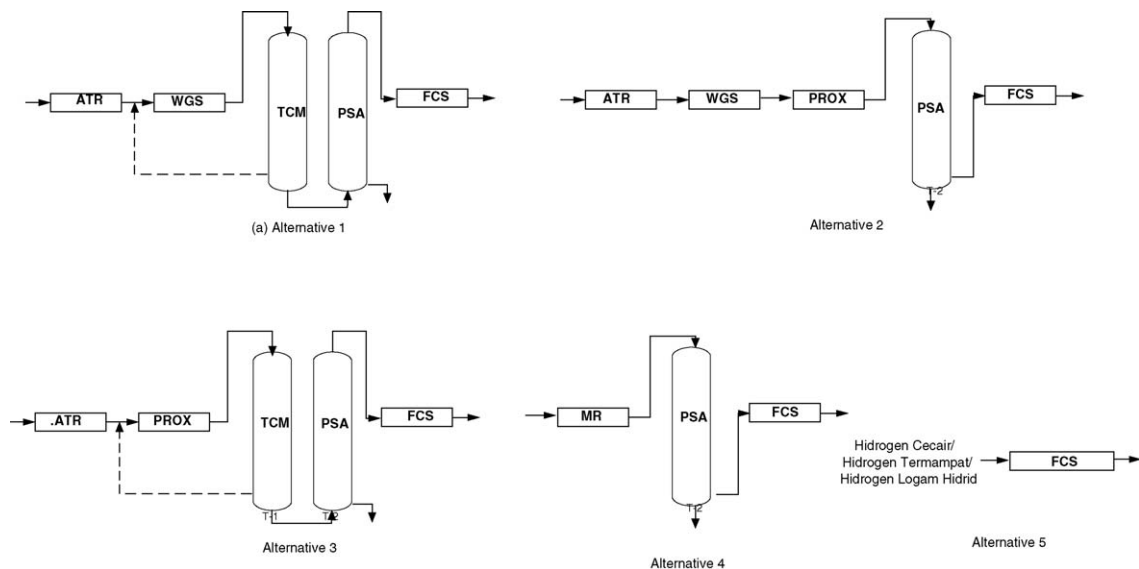

Fig. 3. Four structural alternatives configuration of the units in the system.
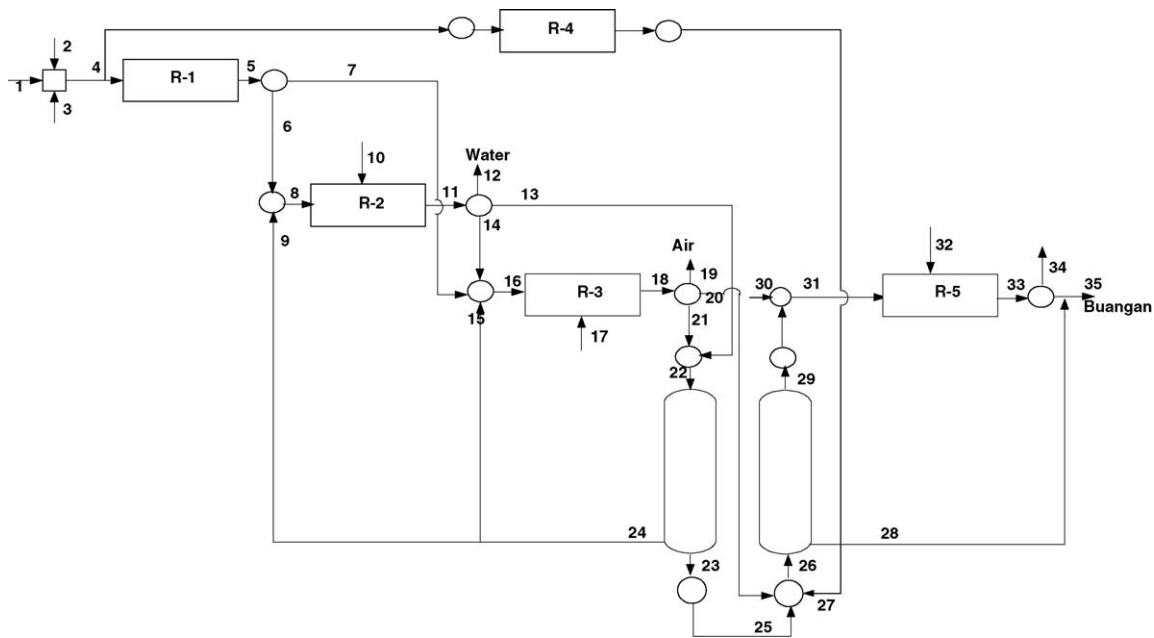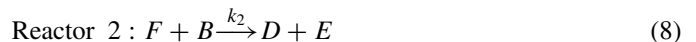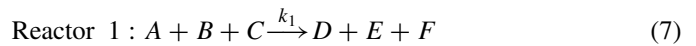
Fig. 4. Superstructure.

The following paragraph presents the mathematical formulation for RSN network by defining the variables for the system:

i. The existence of each unit of reactor and recycle streams (e.g. for NLP problem, the y variable is set to 1 or 0 for the continuous reaction).
ii. The existence of the separation units (e.g. for NLP problem, the z variable is set to 1 or 0 for the separation units).
iii. The stream flow rate (i.e. $F_1, F_2, F_3, \ldots, F_{35}$).
iv. The component compositions (molar fractions) at the inlet of each reactor unit (i.e. $x_{4,i}, x_{6,i}, x_{8,i}, i = A$–$C$) and at the outlet of each reactor unit (i.e. $x_{5,i}, x_{7,i}, x_{9,i}, i = A$–$C$).
v. The volume of the reactor units (i.e. $V_{R,1}, V_{R,2}, V_{R,3}$).
vi. The feed flow rate of components A–C and the final flow rate of components, D–F.
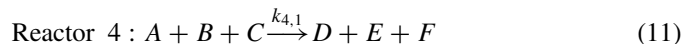vii. The component composition at the inlet of TCM (i.e. $x_{22,i}$, $i = B, D, E, F$).

The set of constraints consists of

i. mass balances for splitters of feed and reactor units;
ii. component balances for mixers at the inlets of the reactor units;
iii. component balances for mixers at the inlet of TCM and PSA;
iv. component balances at the mixers prior to recycles alternatives;
v. component balances around each reactor;
vi. component balance for each separation units;
vii. summation of mole fractions;
viii. logical constraints and volume constraints;
ix. non-negativity and integral constraints.

The reactions involved in the reactor systems are as the following mechanism:

$$\text{Reactor } 1 : A + B + C \xrightarrow{k_1} D + E + F \tag{7}$$

$$\text{Reactor } 2 : F + B \xrightarrow{k_2} D + E \tag{8}$$

$$\text{Reactor } 3 : E + C \xrightarrow{k_{3,1}} F \tag{9}$$

and

$$D + C \xrightarrow{k_{3,2}} B \tag{10}$$

$$\text{Reactor } 4 : A + B + C \xrightarrow{k_{4,1}} D + E + F \tag{11}$$

and

$$F + B \xrightarrow{k_{4,2}} D + E \tag{12}$$

$$\text{Reactor } 5 : D + C \xrightarrow{k_5} B \tag{13}$$

where D is the desired product, A–C are the feed and E and F are the by-product.

Table 3 shows the kinetic constants for the reactions involved, while Table 4 presents the summary of the shortcut design method models used for the design of various units in the system. More detailed information can be found in the cited references. Besides that, Table 5 summarizes the operating conditions for each unit in the system, meanwhile Table 6 shows the cost parameter for the components in the system.

5.1. The objective function

From the overall reactions, D (H_2) is the desired product, A (methanol), B (water/steam), C (O_2) are the feed and E (CO_2) and F (CO) are the by-products. The objective is to minimize

Table 3
Activation energy, pre-exponential factors and reaction constants

Equations	Values
$-r_{ATR} = k_1 C_{M0}^{1.75} \frac{(1-X_M)(M_S-X_M)^{0.5}(M_0-X_M)^{0.25}}{\psi(1+\varepsilon_M X_M)^{1.75}}$	ATR [19] • $E_a = 100.9\,kJ\,mol^{-1}$ • $A_0 = 1.9 \times 10^{12}$ $mol(min\,gcat\,kPa)^{-1}$
$-r_{WGS} = k_2 C_{CO0}^2 \frac{(1-X_{CO})(M'_S - X_{CO})}{(1+\varepsilon_W X_{CO})^2}$	WGS [20] • $E_a = 50\,kJ\,mol^{-1}$ • $A_0 = 1.3 \times 10^7$ $mol(min\,gcat\,kPa)^{-1}$
$r_3 = \frac{k_{CO}k_{O_2} P_{CO} P_{O_2}^n}{0.5.k_{CO} P_{CO} + k_{O_2} P_{O_2}^n}$	PROX [21] • k_{CO} • $E_a = 52.2\,kJ\,mol^{-1}$ • $A_0 = 8.6 \times 10^8$ $mol(min\,gcat\,kPa)^{-1}$ • k_{O_2} • $E_a = 6.02\,kJ\,mol^{-1}$ • $A_0 = 1.75 \times 10^7$ $mol(min\,gcat\,kPa)^{-1}$
$r_4 = \frac{(k_{aCO}/1 + K_D K_{CO} p_M/p_{H_2}^2)(K_D p_M/p_{H_2}^2 - p_{CO})}{\alpha}$	Membrane reactor [22] • $k_{aCO} = 7.7 \times 10^{-10}$ $mol\,cm^{-3}\,s\,atm$ • $K_{CO} = 5.77 \times 10^{-3}\,atm^{-1}$ • $K_D = 76.3\,atm^2$

Table 4
Shortcut design models

Units	Models
ATR [23]	Plug flow reactor: adiabatic and non-isothermal
WGS [23]	Plug flow reactor: isothermal
PROX [21]	Plug flow reactor: isothermal
TCM [24]	The length of the membrane is simplified to number of unit (NTU) and height of transfer unit (HTU)
PSA [25]	The PSA is simplified by using the Klinkenberg solution and introducing Daud bed utilization factor
Stack [26]	Mass balance and the polarization parameter

Table 5
System operating condition for base-case scenario

Parameter	Values
Reformer temperature	250 °C
Reformer pressure	2 bar
Feed flowrate of MeOH	4 mol min^{-1}
MeOH:steam	1:1.3
MeOH:O$_2$	1:0.25
WGS temperature	250 °C
WGS pressure	5 bar
CO:steam	1:30
TC membrane temperature	250 °C
TC membrane H$_2$ outlet temperature	1 bar
PSA temperature	70 °C
PSA pressure	6 bar
Stack pressure	2 bar
Stack temperature	70 °C
H$_2$/O$_2$ ratio in the stack	1.5

Table 6
Cost parameter [27–29]

Components	Cost (US$)/unit
Methanol	$0.08\,g\,mol\,s^{-1}$
ATR	$29.5 \times V_{ATR}^{0.6} \times f_p \times f_m \times I_{kos}$
WGS	$29.5 \times V_{WGS}^{0.6} \times f_p \times f_m \times I_{kos}$
PROX	$29.5 \times V_{PROX}^{0.9} \times f_p \times f_m \times I_{kos}$
TCM	$(0.93/n^{0.7}) \times m \times f_p \times I_{kos}$
Pd MR	$1000 \times V^{0.6} \times I_{kos}$
PSA	$1.54 \times 10^{-3} \times L^{0.81} \times D^{1.05} \times f_p \times I_{kos}$
Water adsorber	$1.54 \times 10^{-3} \times L^{0.81} \times D^{1.05} \times f_p \times I_{kos}$
Air purifier	$1.68 \times 10^{-3} \times L^{0.78} \times D^{0.98} \times f_p \times I_{kos}$
Compressor	$18.5 \times P^{0.77} \times f_{jenis} \times I_{kos}$
Heat exchanger	$3.3 \times A^{0.0024} \times I_{kos}$
Pump	109
Stack	$0.35\,m^{-2}$

	Investment cost (US$ × 10^3)
ATR	$93.4 \times V_1$
WGS	$145 \times V_2$
PROX	$160 \times V_3$
TCM	$2116.8 \times$ feed flow rate
PSA	$39 \times$ feed flow rate
Air purifier	$39 \times$ feed flow rate
Water adsorber	$39 \times$ feed flow rate
Compressor	$58.6 \times P_m$
Stack	$440 \times W$

the cost and the production of E. The total investment cost, C_T is given as below:

Total cost,

$$C_T = C_A + C_B + C_C + C_{R-1} + C_{R-2} + C_{R-3} + C_{R-4} + C_{S-1} + C_{S-2} + C_{Utilities} \tag{14}$$

$$C_A = F_1 \times 0.08 \times 9.56 \times 10^6 \tag{15}$$

$$C_B = 8.0 \times 10^6 \times 6.3 \times (F_2 + F_{10}), \tag{16}$$

$$C_C = 3 \times 13 \times 10^3 (F_3 + F_{17} + F_{30}), \tag{17}$$

$$C_{R-1} = 93.4 \times 10^3 \times V_1 + Q_1, \tag{18}$$

$$C_{R-2} = 145 \times 10^3 \times V_2 + Q_2, \tag{19}$$

$$C_{R-3} = 160 \times 10^3 \times V_3 + Q_3, \tag{20}$$

$$C_{R-4} = F_{29} x_{29,D} \times 9.5 \times 10^6 \tag{21}$$

$$C_{S-1} = F_{22} \times 2116.8 \times 10^3 \tag{22}$$

$$C_{S-2} = F_{26} \times 39 \times 10^3 \tag{23}$$

$$C_{Utilities} = [39 \times 10^3 (F_{12} + F_{19} + F_{32})] + [0.175 \times 10^6 \times 8 \times 330] \tag{24}$$

$$V_1 = \frac{F_1}{\psi\rho(1-\varepsilon)k_1} \int_0^{X_1} \frac{(1+\varepsilon_V X_1)\,dX}{C_{A0}(1-X_1)}; \tag{25}$$

$$V_2 = \frac{F_8 x_{8,F}}{\psi k_2 \rho(1-\varepsilon)C_{F0,8}} \int_0^{X_2} \frac{(1+\varepsilon_W X_2)\,dX}{(1-X_2)}; \tag{26}$$

$$V_3 = \frac{F_{16}x_{16,F}}{\psi k_3 \rho (1-\varepsilon) C_{F0,16}^2} \int_0^{X_3} \frac{(1+\varepsilon_W X_3)^2 \, dX}{(1-X_3)(\lambda - X_3)}; \tag{27}$$

$$Q_1 = F_5 x_{5,D}(7.2) + F_5 x_{5,E}(-291) - [F_1(-201) + F_2(1.3) + F_3(-233)], \tag{28}$$

$$Q_2 = F_{11}x_{11,D}(-359) + F_{11}x_{11,E}(-384) - [F_8 x_{8,F}(-101) + F_{10}(-231)], \tag{29}$$

$$Q_3 = F_{18}x_{18,B}(-12.9) + F_{18}x_{18,E}(-16.8) - [F_{17}(-1.1) + F_{16}x_{16,D}(-10.3) + F_{16}x_{16,E}(-10.6)] \tag{30}$$

$$C_T = \begin{bmatrix} [F_1 \times 7.6 \times 10^5] + [5 \times 10^7 (F_2 + F_{10})] + [3.9 \times 10^4 (F_3 + F_{17} + F_{30})] + [9.4 \times 10^4 V_1 + 96.94 Q_1] \\ + [1.2 \times 10^5 V_2 + 96.94 Q_2] + [1.2 \times 10^5 V_3 + 250 Q_3] + [7 \times 10^8 F_{29}x_{29,D}] + [2 \times 10^6 F_{22}] \\ + [4 \times 10^4 F_{26}] + [4.0 \times 10^4 (F_{12} + F_{19} + F_{32})] + [6 \times 10^9] \end{bmatrix} \tag{31}$$

Fig. 5. Comparison of specific manufacturing and investment.

The mathematical model shown above is an MINLP problem since it has both continuous and binary variables and non-linear objectives and constraints. The binary variables participate linearly in the objective and logical constraints. However, due to
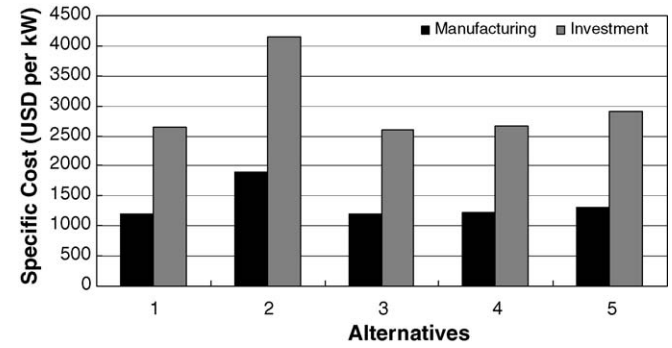
$$[g(X)]_m \leq 0 \tag{34}$$

$$X^{low} \leq X \leq X^{up} \tag{35}$$

With that, the objective function is:

$$\text{Min} f(X) = \begin{bmatrix} 7.6 \times 10^5 x_1 + 5 \times 10^7 x_2 + 5 \times 10^7 x_{14} + 3.9 \times 10^4 x_3 \\ + 3.9 \times 10^4 x_{24} + 3.9 \times 10^4 x_{45} + 9.4 \times 10^4 V_1 + 96.94 Q_1 \\ + 1.2 \times 10^5 V_2 + 96.94 Q_2 + 1.2 \times 10^5 V_3 + 250 Q_2 \\ + 7 \times 10^8 x_{61} x_{98} + 2 \times 10^6 x_{57} + 4 \times 10^4 x_{60} + 4.0 \times 10^4 x_{19} \\ + 4.0 \times 10^4 x_{29} + 4.0 \times 10^4 x_{46} + 6 \times 10^9 \end{bmatrix} \tag{36}$$

6. Result and discussion

The model development for the synthesis and optimization processes in this study was based on the power output, P.

6.1. Process synthesis

Five chosen alternatives are used in the synthesis process, as explained in Section 5. The summarized results for the synthesis and optimization processes are as given in Table 6.

Figs. 5–7 are plotted based on the results from Table 7. Figs. 5 and 6 show that the alternative 2 gives the highest specific manufacturing and investment costs up to US$ 4000 and 1900,

the complexity of the MINLP, the problem is solved using the NLP, where it considers only the continuous variables while the binary variables $\{y, z\}$ are set to 0 or 1. Constraints (i), (vii) and (viii) are linear while the remaining constraints are non-linear. The non-linearity in constraints and objectives function is bilinear type.

Design parameters:

$k_1, k_2, k_3 \eta_{fuelcell}, \rho, \varepsilon, \psi, S_1, S_2, S_3, S_4, \lambda, \theta, \dfrac{c}{c_F},$

$V, I_n, I, \eta, P, T_1, T_2, T_3, P_1, P_2, P_3, w, L$

Design variables:

$F_1, F_2, \ldots F_{33}, x_{1,i}, x_{2,i} \ldots x_{33,i}, V_1, V_2, V_3, Q_1, Q_2, Q_3,$

$A_M, A_A, A_F,$

where $i = A$–F.

Associating the design variable x_1–x_{87} with $F_1, F_2, \ldots F_{33}$, $x_{1,i}, x_{2,i} \ldots x_{33,i}, V_1, V_2, V_3, Q_1, Q_2, Q_3, A_M, A_A, A_F$. Then the problem can be expressed as the following:

Minimize $\quad f(X), [X]_n \tag{32}$

s.t.:

$[h(X)]_l = 0 \tag{33}$
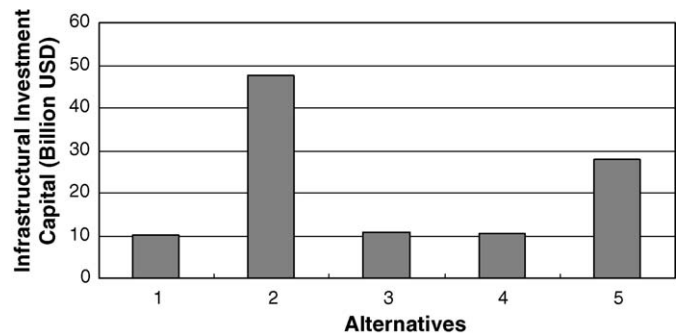

Fig. 6. The comparison of infrastructural investment capital.
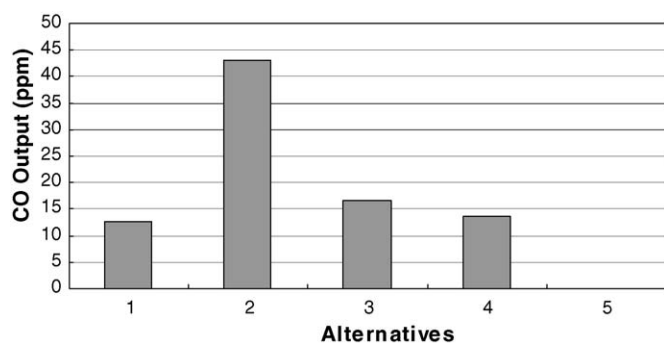
Fig. 7. The comparison of output CO concentration.

Table 8
Input and output parameter for 5 kW power output (alternative 1)

Parameters	Values
Net power output (kW)	2.38
System efficiency (%)	47.57
Methanol input ($l\,min^{-1}$)	87.3
Water input ($l\,min^{-1}$)	113
Oxygen input ($l\,min^{-1}$)	21.8
Concentration of CO output (ppm)	12.6

respectively, whereas the alternatives 1, 3, 4 and 5 give lower costs in the range of US$ 2600–3000 and 1200–1500 kW^{-1}, respectively. This is because of the larger cost of the PROX reactor obtained compared to those of the ATR and the WGS reactors as the catalyst for the PROX reaction is very selective and expensive.

In Fig. 6, it is observed that the cost calculations for the infrastructural investment for alternative 2 comes up with a figure amounting to US$ 48 billion while the figures for alternatives 1, 3, 4 and 5 are only in the range of US$ 10–30 billion (Fig. 6). As the main objective of the synthesis is to minimize its investment cost as well as the carbon monoxide production, the next selection has to be based on the CO output. From Fig. 7, alternative 1 gives the lowest CO output, i.e. 12.6 ppm, followed by alternative 4 (included a membrane reactor unit), i.e. 13.5 ppm, and alternative 3 of 16.5 ppm. On the contrary, alternative 5 gives zero CO output because only hydrogen and oxygen are used as its feed without any hydrocarbon component. Besides the highest cost that the alternative 2 incurs, it also produces the highest CO content of 43.1 ppm, causing it to be eliminated from the selection.

Therefore, alternative 1 is the best choice because it gives lower CO output and specific manufacturing and investment costs compared to the other three alternatives. Although alternative 5 gives a zero CO output but its specific manufacturing and investment costs as well its infrastructural investment cost are too high, i.e. US$ 1350, 2950 and 28 billion, respectively, compared to the ones incurred by alternative 1, i.e. US$ 1200, 2600 and 10 billion, respectively.

6.2. Optimization

Table 8 presents the summarized results after optimization for alternative 1 with power output of 5 kW, with reference to the operation parameters in Table 5, while Tables 9 and 10 give the detailed design and economic parameters.

From the synthesis and optimization processes, the following has been identified in this study:

- The WGS reaction is required in a fuel cell system as the primary CO remover, followed by the membrane or PROX reaction that acts as the secondary CO remover along with an adsorbent system. This finding repudiates earlier statements from [19,30], which claim that the WGS reactor is not required as one of the CO removal systems in the fuel processing unit because the main problem with the WGS reactor is the low operating temperature and the large reactor size. Instead, it agrees with the study put forth by refs. [31–34], which prove that the WGS reaction is an integral part of the PEMFC system as a CO removal unit and a secondary source of hydrogen. Apart from that, this study has also identified that the operating pressure can be used to control the size of the WGS reactor [23].

- This study has also proven that the combined WGS-membrane reaction works better and is more cost-effective compared to the one by the PROX-membrane combination. This is because the reaction and effectiveness of the PROX reactor are very much dependent on the choice of catalyst with a high CO oxidation selectivity and this type of catalyst is expensive. The catalyst for the PROX reaction has characteristics that prevent H_2 selection by CO oxidation but H_2 oxidation will take over when the partial pressure of CO

Table 7
Summarized result from process synthesis

Parameters	1	2	3	4	5
Power output (kW)	5	5	5	5	5
Net power output (kW)	2.38	2.38	2.38	2.38	3.25
System efficiency (%)	47.57	47.57	47.57	47.57	65.0
Methanol input ($l\,min^{-1}$)	87.3	92.3	35.5	96.7	0
Water input ($l\,min^{-1}$)	113	120	46.1	145	0
Oxygen input ($l\,min^{-1}$)	21.8	23.1	8.87	32.9	125
CO output (ppm)	12.6	43.1	16.5	13.5	0
Working capital (US$)	1980	3108	1956	2000	1516
Specific manufacturing cost (US$ kW^{-1})	1210	1900	1194	1220	1347
Specific investment cost (US$ kW^{-1})	2639.6	4144.1	2608.2	2665.7	2942.2
Infrastructural investment capital (billion US$)	10.3	47.7	10.5	10.7	28

Table 9
Detailed design parameters (alternative 1)

Parameters	Value
ATR	
Pressure (bar)	1
Temperature ($^\circ$C)	250
Conversion (%)	98.7
Reactor volume (cm^3)	148
Catalyst density (m^3 kg^{-1})	1.1
Voidage	0.5
Rate constant (mol kg^{-1} s^{-1})	0.038
WGS	
Pressure (bar)	5
Temperature ($^\circ$C)	220
Conversion (%)	90.6
Reactor volume (cm^3)	325
Catalyst density (m^3 kg^{-1})	1.1
Voidage	0.5
Rate constant (mol kg^{-1} s^{-1})	0.091
TCM	
Inlet pressure, PM1 (bar)	5
Outlet pressure, PM2 (bar)	1
$r = $ PM2/PM1	0.2
Temperature ($^\circ$C)	250
Degree of separation	0.3
Pore diameter (nm)	1.5
Membrane thickness (m)	0.0005
Membrane module diameter (m)	0.15
Membrane length (m)	0.36
PSA	
Pressure (bar)	6
Temperature ($^\circ$C)	25
Separation factor (c/c_F)	0.01
Daud utilization factor (δ)	0.2
Superstantial velocity (cm s^{-1})	5
Equilibrium constant	6500
Mass transfer constant (cm^{-1})	0.02
Bed diameter (m)	0.10
Bed length (m)	0.177
Breakthrough time (s)	3.3
FCS	
Single cell voltage (V)	0.7
Current (A)	200
Number of cell	36
Current density (A cm^{-2})	0.8
Cell active area (cm^2 per cell)	250
Length (cm)	15.8
Width (cm)	15.8

Table 10
Economic parameters

Components	Cost (US$)
ATR	133.9
WGS	214.8
Compressor	370.0
Fuel feeding pump	106.0
Recycle pump	106.0
TCM	372.2
PSA	16.8
Air purifier	6.9
Water separator	10.5
Heat exchanger unit	389.0
PEMFC stack	2678.6
Manufacturing cost	6043.1
Installation cost	9064.7
Coat for 1 unit of PEM fuel	13198.1
Specific manufacturing cost	1208.6 kW^{-1}
Specific investment cost	2639.6 kW^{-1}
Infrastructural investment capital	10.3 billion
Electricity cost	0.04 kWh

Table 11
Comparison Of feed flow rate of methanol with other studies

References	Power output (P, kW)	Value (1 h^{-1})
[30]	5	1.44
[23,26] (before optimization)	5	1.86
This study (after optimization)	5	1.42

decreases. In practice, the reaction of PROX selection for the CO oxidation will be more difficult with the decrease in CO concentration [19,21,35]. In addition, the combined PROX-membrane reaction will incur a higher cost, i.e. two times more, compared to the one by the WGS-membrane combination.

- From this study, the pressurized oscillation adsorbent system, PSA, is found to be essential in CO removal before the flow enters the fuel cell stack. This is because the PSA is very efficient in terms of product purity, product cost, operating cost and capital cost as proven by refs. [36,37]. Even though the PSA design is complicated with large number of parameters that must be considered throughout, this has been successfully overcome by introducing a simple, short cut design method for the PSA [23].

- The membrane reactor system (alternative 4) is also a very suitable consideration for the fuel cell system because it gives highly similar performance and cost comparisons to alternative 1. In addition, it can produce smaller, more compact, and lighter fuel cell system as suggested by refs. [22,38,39].

6.3. Model verification

In general, validation for the models developed for process synthesis and optimization is carried out based on other studies and the model development with Microsoft Excel before optimization [23,26].

Table 11 gives the fuel feed value required by the fuel cell system with 5 kW of power output. It is found that this value is

Table 12
The comparison of system efficiency with other studies

References	Efficiency (%)
[40]	32–40
[41]	40–60
[42]	40
[43]	40–60
[44]	40–60
[26] (before optimization)	45.5
This study (after optimization)	47.5

Table 13
The comparison of specific stack cost with other studies

References	System	Cost per kW (US$)
[42]	PEMFC	500–800
[48]	PEMFC	500–1000
[43]	PEMFC	400–1000
[49]	PEMFC	750–1000
[45]	PEMFC	200–300
[46]	PEMFC	400–700
This study	PEMFC	500–700

Table 14
The comparison of specific manufacturing cost with other studies

References	System	Cost per kW (US$)
[40]	PEMFC (light industry)	1000–2000
[48]	PEMFC (vehicles)	1000–2000
This study	PEMFC (vehicles)	1000–1500

comparable to the value obtained by ref. [28]. Meanwhile, the methanol feed value before optimization is at a rate of $1.86 \, l \, h^{-1}$ while after optimization is at the rate of $1.42 \, l \, h^{-1}$. This shows a good improvement of the system after the optimization process.

Table 12 gives the results of the system efficiency obtained in this study as compared to other studies. The system efficiency value in this study is calculated by taking into account the fuel processing system efficiency factor, η_{fp} as 0.95, the separation system efficiency factor η_{sp} as 0.95, the fuel cell stack efficiency factor, η_{fc} as 0.65 and the parasitic load as 8% of the output power. The system efficiency value in this study is found to be within the range obtained by other studies. Apart from that, the system efficiency was observed to have increased from 45.5% before optimization to 47.5% after optimization.

The next paragraph explains on model verification for economic parameters. It is found that the value of the specific stack cost incurred by this study is in the range of US$ 500–700. This value is comparable to the ones obtained by other studies as shown in Table 13. However, the model given by ref. [45] expects the cost to be as low as US$ 200–300 kW^{-1}. This is because the cost shown is referred to a high output capacity of up to 500,000 vehicle units. Therefore, it can be deduced that cost-saving effort is very much dependent on the output capacity. This has been put forth in a study by ref. [46], which predict that the fuel cell cost in the year 2020 will be at a rate of US$ 38 kW^{-1} with an annual output capacity of 5 million fuel

Table 15
The comparison of specific investment cost with other studies

References	System	Cost per kW (US$)
[47]	PEMFC	2600–3000
[44]	PEMFC	2500–3000
[50]	PAFC	3000
[51]	PEMFC	2500
[29]	SOFC	2500–3000
[52]	PEMFC	2000–3000
This study	PEMFC	2500–3000

Table 16
Infrastructural investment cost

References	Vehicles capacity production (million)	Infrastructural investment cost (billion US$)	Vehicle cost (US$ per kW)
[47]	25 (methanol–H_2)	45–95	2000–3800
This study	5 (methanol–H_2)	10–20	2000–4000

cell vehicles. The estimated specific manufacturing and investment costs obtained by other studies are in the range given in Tables 14 and 15. The infrastructural investment cost is as shown in Table 16. The infrastructural investment cost in this study is in the range of US$ 10–30 billion with an output capacity of 5 million and a cost of US$ 2000–4000 kW^{-1}. This is comparable to the study by ref. [47].

7. Conclusions

The main objective of this study, which was to solve the synthesis and optimize the design for a PEM fuel cell system via a separator-reactor using the SQP approach for non-linear equations, was successfully obtained. Although the non-linear SQP approach is a well-known method in chemical system designs, this study is the first attempt for a fuel cell system. The complex equations involved have been simplified into matrix forms and solved using MATHLAB software.

Acknowledgements

References

[1] T.F. Yee, I.E. Grossmann, Simultaneous optimization models for heat integration -II. Heat exchanger network synthesis, Comput. Chem. Eng. 14 (1990) 1165.

[2] B. Linhoff, V.R. Dhole, Shaft work targets for low-temperature process design, Comput. Chem. Eng. 47 (8) (1992) 2081–2091.

[3] K.P. Papalexandri, E.N. Pistikopoulos, A Multi period MINLP model for the synthesis of flexible heat and mass exchange networks, Comput. Chem. Eng. 18 (11/12) (1994) 1125–1139.

[4] N.B. Vaklieva, B.B. Ivanov, N. Shah, C.C. Pantelides, Heat exchanger network design for multipurpose batch plants, Comput. Chem. Eng. 20 (8) (1996) 989–1001.

[5] X.G. Zhao, B.K. O'Neill, J.R. Roach, R.M. Wood, Heat integration for batch processes. Part 2: heat exchanger network design, Trans. IChemE 76 (A) (1998) 700–710.

[6] B. Linnhoff, H. Dunford, R. Smith, Heat integration of distillation columns in overall processes, Chem. Eng. Sci. 38 (1973) 1175.

[7] C.A. Floudas, G.E. Paules, A Mixed-integer nonlinear programming formulation for the synthesis of heat-integrated distillation sequences, Comput. Chem. Eng. 12 (1988) 531.

[8] J.E. Hansen, S.B. Jørgensen, J. Heath, J.D. Perkins, Control structure selection for energy integrated distillation column, J. Process Control 8 (3) (1998) 85–195.

[9] K. Liebmann, R.V. Dhole, M. Johnson, Integrated design of a conventional crude oil distillation tower using pinch analysis, Inst. Chem. Eng. 76 (A) (1998) 335–547.

[10] M.J. Andrecovich, A.W. Westberg, A simple synthesis method based on utility bounding for heat integrated distillation sequences, AIChE J. 31 (1985) 363.

[11] C.A. Floudas, Nonlinear and Mixed-Integer Optimization, Oxford University Press, New York, 1995.

[12] T.L. Biegler, E.I. Grossman, W.A. Westerberg, Systematic Method of Chemical Design, International Edition, Prentice hall International, Inc., New Jersey, 1997.

[13] K. Shivakumar, S. Narasimhan, A robust application and efficient NLP formulation using graph theoretic principle for syntheses of heat exchanger networks, Comput. Chem. Eng. 26 (2002) 1517–1532.

[14] J.S. Buouerouf, L.T. Biegler, Decomposition algorithms for on-line estimation with nonlinear models, Comput. Chem. Eng. 19 (10) (1995) 1031–1039.

[15] J.V.P. Barbosa, M.R.M. Wolf, F.R. Maciel, Development of data reconciliation for dynamic nonlinear system: application the polymerization reactor, Comput. Chem. Eng. 21 (2000) 501–506.

[16] G.C. Itle, A.G. Salinger, R.P. Pawlowski, J.N. Shadid, L.T. Biegler, A tailored optimization strategy for PDE-based design application to a CVD reactor, Comput. Chem. Eng. 28 (2004) 291–302.

[17] J. David, L.T. Biegler, Interior-point methods for reduced Hessian successive quadratic programming, Comput. Chem. Eng. 23 (7) (1999) 859–873.

[19] J. Agrell, H. Birgersson, M. Boutonnet, Steam reforming of methanol over a $Cu/ZnO/Al_2O_3$ catalyst: a kinetic analysis and strategies for the suppression of CO formation, J. Power Sources 46 (2002) 1–9.

[20] P. Mizsey, E. Newson, T.H. Truong, P. Hottinger, The kinetic of methanol decomposition: a part of autothermal partial oxidation to produce hydrogen for fuel cells, Appl. Catal. A: Gen. 213 (2001) 233–237.

[21] G. Sedmak, S. Hocevar, J. Levec, Kinetics of selective CO oxidation in excess of H_2 over the nanostructured $Cu_{0.1}$, $C_{0.9}$ O_{2-y} catalysts, J. Power Sources 213 (2003) 135–150.

[22] M.P. Harold, B. Nair, G. Kolios, Hydrogen generation in a Pd membrane fuel processor: assessment of methanol-based reaction system, Chem. Eng. Sci. 58 (2003) 2551–2571.

[23] S.K. Kamarudin, W.R.W. Daud, A. MdSom, A.W. Mohammad, S. Takriff, Y.K. Loke, Design of a fuel processor unit for PEM fuel cell via shortcut design method, Fuel Cell Virtual J. 2 (12) (2005), http://www.elsevier.com/wps/find/P04.cws_home/vj_fuel_cell_archive.

[24] S.K. Kamarudin, W.R.W. Daud, A. Md. Som, A.W. Mohammad, Takriff, Design of a tubular ceramic membrane for gas separation in a PEMFC system, J. Fuel Cell: Syst. Fund. 3 (4) (2003) 189–198.

[25] W.R.W. Daud, Prinsip Reka bentuk Process Kimia, Institusi Jurutera Kimia Malaysia, Bangi, 2002.

[26] S.K. Kamarudin, W.R.W. Daud, A. Md. Som, A.W. Mohammad, S. Takriff, M. Masdar, The conceptual design of PEMFC system via simulation, Chem. Eng. J. 103 (1–3) (2004) 99–113.

[27] J.M. Ogdean, R.H. Williams, E.D. Larson, Societal lifecycle costs of cars with alternative fuels/engines, Energy Policy 32 (1) (2004) 7–27.

[28] H.D. Geol, J. Grievink, P.M. Herder, M.P.C. Weijin, Integrating reliability optimization into chemical process synthesis, Reliability Eng. Syst. Saf. 78 (2002) 247–258.

[29] F. Baratto, U.M. Diwekar, D. Manca, Impact assessment and tradeoff of fuel cell based auxiliary power units. Part II. Environmental and health impacts, LCA and multi objective optimisation, J. Power Sources 139 (2005) 214–222.

[30] L. Ma, D.L. Trimm, C. Jiang, The design and testing of an auto-thermal reactor for the conversion of light hydrocarbons to hydrogen i. the kinetics of the catalyst oxidation of light hydrocarbons, Appl. Catal. A: Gen. 138 (1996) 275–283.

[31] S. Giessler, L. Jordan, G.Q. Lu, Performance of hydrophobic and hydrophilic silica membrane reactors for the water gas shift reaction, Sep. Purif. Technol. 32 (1–3) (2003) 255–264.

[32] D.R. Palo, J.D. Holladay, R.T. Rozimiarek, C.E.G. Leong, J. Wang, J. Hu, Y.H. Chin, R.A. Dagle, E.G. Baker, Development of a soldier-potable fuel cell power system, J. Power Sources 108 (2002) 28–34.

[33] A.Y. Tonkovich, J.L. Zilka, M.J. Lampunt, Y. Wang, R.S. Wegeng, Micro channel reactors for fuel cell processing application. I. Water gas shift reactor, Chem. Eng. Sci. 54 (1999) 2947–2951.

[34] J.M. Zalc, D.G. Loffler, Fuel Processing for PEM fuel cells: transport and kinetics issues of system design, J. Power Sources 48 (2002) 1–7.

[35] F. Mariño, C. Descorme, D. Duprez, Noble metal catalysts for the preferential oxidation of carbon monoxide in the presence of hydrogen (PROX), Appl. Catal. B: Environ. 54 (1) (2004) 59–66.

[36] S.E. Iyuke, W.R.W. Daud, A.B. Mohammad, A.A.H. Kadhum, Z. Fisal, A.M. Shariff, Application Of Sn-activated carbon in pressure swing adsorption for purification on H_2, Chem. Eng. Sci. 55 (2000) 4745–4755.

[37] S. Jain, A.S. Moharir, P. Li, G. Wozny, Heuristic design of pressure swing adsorption: a preliminary study, J. Sep. Purif. Technol. 33 (2003) 25–43.

[38] J. Balster, D.F. Stamatialis, M. Wessling, Electro-catalytic membrane reactors and the development of bipolar membrane technology, Chem. Eng. Process. 43 (9) (2004) 1115–1127.

[39] J.R. Lattner, M.P. Harold, Comparison conventional and membrane reactor fuel processor for hydrocarbon-based PEM fuel cell system, Int. J. Hydrogen Energy 29 (2004) 393–417.

[40] A.U. Dufour, Fuel cells—a new contributor to stationary power, J. Power Sources 71 (1998) 19–25.

[41] D. Xue, Z. Dong, Optimal fuel cell system design considering functional performance and production costs, J. Power Sources 76 (1998) 69–80.

[42] N.M. Sammes, R. Boersma, Small scale fuel cells for residential applications, J. Power Sources 86 (2000) 98–110.

[43] G. Cacciola, V. Antonucci, S. Freni, Technology up date and new strategies on fuel cells, J. Power Source 100 (1–2) (2001) 67–79.

[44] A. Kazim, Exergo-economic analysis of a PEM fuel cell at various operating conditions, Energy Convers. Manag. 46 (7–8) (2005) 1073–1081.

[45] I. Bar-Onn, R. Kirchain, R. Roth, Technical cost analysis for PEMFCs, J. Power Sources 4759 (2002) 1–5.

[46] H. Tscuchiya, O. Kobayashi, Mass Production cost of PEM fuel cell by learning curve, Int. J. Hydrogen Energy 29 (2004) 985–990.

[47] W.P. Teagen, J. Bently, B. Barnett, Cost reduction of fuel cells for transportation applications: fuel processing options, J. Power Sources 71 (1998) 80–85.

[48] G. McKerron, Financial considerations of exploiting fuel cell technology, J. Power Sources 86 (2000) 28–33.

[49] C. Bernay, M. Marchand, M. Cassir, Prospects of different fuel cell technologies for vehicle application, J. Power Sources 108 (1–2) (2002) 139–152.

[50] H.Y. Kwak, H.S. Lee, J.Y. Jung, J.S. Jeon, D.R. Park, Exegetic and thermoeconomic analysis of a 200 kW phosphoric acid fuel cell plant, Fuel 83 (2004) 2087–2094.

[51] A. Kazim, Exergy analysis of a PEM fuel cell at variable operating condition, Energy Convers. Manag. 45 (2004) 1949–1961.

[52] R. Roy, S. Colmer, T. Griggs, Estimating the cost of a new technology intensive automotive product: a case study approach, Int. J. Prod. Econ. 97 (2) (2004) 210–226.